Precise electroosmotic flow measurements on paper substrates

Nicolás Franck[1], Federico Schaumburg[2], Pablo A. Kler[1,3], and Raúl Urteaga[4]

[1]CIMEC (Universidad Nacional del Litoral–CONICET), Colectora RN 168 Km 472, S3000GLN Santa Fe, Argentina.
[2]INTEC (Universidad Nacional del Litoral–CONICET), Colectora RN 168 Km 472, S3000GLN Santa Fe, Argentina.
[3]Departamento de Ingeniería en Sistemas de Información, FRSF-UTN., Lavaise 610, S3004EWB Santa Fe, Argentina.
[4]Instituto de Física del Litoral (IFIS Litoral, UNL–CONICET)., Guemes 3450, S3000GLN Santa Fe, Argentina.

Prof. Dr. Raúl Urteaga
Instituto de Física del Litoral

UNL–CONICET
Güemes 3450
S3000GLN Santa Fe, Argentina
Tel.: +54-342-45119174
Fax: +54-342-4550944
urteagar@santafe-conicet.gov.ar

Prof. Dr. Pablo A. Kler
Centro de Investigación
de Métodos Computacionales
UNL–CONICET
Predio Dr. Alberto Cassano RN168 km 473
S3000GLN Santa Fe, Argentina
Tel.: +54-342-4511594
Fax: +54-342-4511169
kler@cimec.santafe-conicet.gov.ar

List of abbreviations:

µPAD	Microfluidic paper-based analytical device
e-µPAD	Electrophoretic microfluidic paper-based analytical device
EOF	Electroosmotic flow
IEF	Isoelectric Focusing
POC	Point of Care
ZE	Zone electrophoresis

Keywords: Paper-based microfluidics; Electrophoresis; Electroosmosis; Whatman #1;

Abstract

A novel method for electroosmotic flow (EOF) measurement on paper substrates is presented; it is based on dynamic mass measurements by simply using an analytical balance. This technique provides a more reliable alternative to other EOF measurement methods on porous media. The proposed method is used to increase the amount and quality of the available information about physical parameters that characterize fluid flow on microfluidic paper–based analytical devices (µPADs). Measurements were performed on some of the most frequently used materials for µPADs, i.e. Whatman #1 , S&S and Muntktell 00A filter paper. Obtained experimental results are consistent with the few previously reported data, either experimental or numerical, characterizing EOF in paper substrates. Moreover, a thorough analysis is presented for the quantification of the different effects that affect the measurements such as Joule effect and evaporation. Experimental results enabled, for the first time, to establish well defined electroosmotic characteristics for the three substrates in terms of the magnitude of EOF as funtion of pH, enabling researchers to make a rational choice of the substrate depending on the electrophoretic technique to be implemented. The measurement method can be described as robust, reliable, and affordable enough for being adopted by researchers and companies devoted to electrophoretic µPADs and related technologies.

1 Introduction

Paper-based electrophoretic separations have renewed its relevance due to the contemporary expansion of paper-based microfluidic analytic devicess (µPADs)[1]. Although several attempts were made in the mid 20th century for the separation of serum proteins [2, 3], and small inorganic molecules [4, 5], the advantages later shown by capillary and gel-based separations interrupted the development of such techniques in paper substrates, for more than 70 years.

Hence, several research groups began developing electrophoretic µPADs (e-µPADs) in the last years. Paper-based electrophoretic separations have been demonstrated with different results in terms of separation efficiency and detection limits. For example paper zone electrophoresis has been proven for amino-acids [6] and small inorganic molecules [7, 8] as well as isotachophoresis for increasing the efficiency of lateral flow analysis [9, 10]. However, µPADs in general and e-µPADs in particular suffer from poor repeatably, preventing this technology from finding new applications in sensitive fields like point-of-care (POC) or food safety. Such lack of reproducibility, is attached to the high scatter of the physical parameters that describe the substrates, and determine their behavior under fluid flow, mass transport and electric field actions [11, 12]. These parameters are the porosity (ϕ), tortuosity (τ), permeability (K), dispersion coefficient (s), and electroosmotic mobility (K_{eo}) [13, 14]. Although a detailed knowledge of the substrates seems to be necessary to develop reliable devices, little effort has been done to characterize the the most common paper types used in e-µPADs. The aforementioned set of parameters can be split into two groups. On one hand ϕ, K, and s are consistently informed with a remarkable reproducibility. On the other hand τ and K_{eo} are scarcely reported and with significant dispersion over their numerical values. Although this work focuses on K_{eo}, it is also of critical importance to develop similar studies on τ.

On a general basis, K_{eo} can be defined as the ratio between the mean electroosmotic velocity u_{eo} and the electric field E, i.e. [15],

$$K_{eo} = \frac{u_{eo}}{E}. \tag{1}$$

For non-porous media (tipically capillary tubes or microchannels), when the electric double layer is thin compared to the width of the channel, K_{eo} is given by the Helmholtz-Smoluchowski relation [16]:

$$K_{eo} = -\frac{\epsilon\zeta}{\mu} \tag{2}$$

where ϵ and μ represent the electrical permittivity and viscosity of the solvent, while ζ represents the electrokinetic potential, i.e. the potential difference across the electric double layer, which depends on the material of the wall, polarity of the solvent, and, ionic strength and pH of the electrolyte solution [17].

In contrast to equation 2, extensively validated for capillary and microchip electrophoretic separations [18], there are only a few models of K_{eo} for porous media, mainly based on modelling the paper substrate as a bunch of non-interconnected capillary tubes [12, 15, 19]. In such models, the ζ-potential associated to electroosmotic flow (EOF) in paper substrates (ζ_p) plays the role of an operational parameter, whose value condenses most of the assumptions performed by such models. Recently, Schaumburg et al. presented a comprehensive model for electromigrative phenomena in paper-based substrates [12]. This model considers the e-µPADs material as a set of tortuous capillaries, with a preferential direction for the flow and with an equivalent section along the flow for each capillary. Using this model it is possible to arrive to an expression for K_{eo}; by considering the pressure gradient negligible, as it is the case of pure EOF on a single paper strip (which is also the case of our experimental setup) such expression is:

$$K_{eo} = -\frac{\phi\epsilon\zeta_p}{\tau^2\mu}. \tag{3}$$

Thus, K_{eo} can be obtained from ζ_p provided that parameters characteristic of the substrate and the fluid are known. It that regard, Schaumburg et al. validated their model with a ZE experiment from literature, using $\tau = 2.9$ and $\zeta_p = -15\,\mathrm{mV}$ for Whatman # 1 filter paper, although parameters were reported with a level of uncertainty higher than 50 %. Similarly, the scarce ζ_p values reported calculated using other porous media models, also show great scatter. For instance, Rosenfeld and Bercovici [19] obtained $\zeta_p = -45\,\mathrm{mV}$ starting from an EOF measurement

in nitrocellulose at $pH = 8$. Also, Leung [20] obtained $\zeta_p = -12.5 \pm 6.5\,\text{mV}$ when $pH = 3.7$ for Whatman #1 paper using a fiber-pad streaming potential technique. To the best of our knowledge, the rest of the reported numerical values for EOF characterization were obtained using the electric current monitoring method for Whatman #1 or other filter paper with similar pore sizes [3, 21, 22]. Different from capillaries or microchannels, using the electric current method for EOF measurement in paper substrates is challenging and suffers from poor reproducibility. The uncertainty and scatter of informed ζ_p and K_{eo} values show that substrate characterization is still not up to the requirements of rational design of e-µPADs . The aforementioned problem uncovers the need of a unique and accepted model for e-µPADs to enable researchers to associate EOF with an intrinsic ζ-potential at the solid-liquid interface in the microscopic level, and the need of a reliable and robust method for the quantification of EOF in e-µPADs for direct estimation of K_{eo}.

Consequently, in this work we present a reliable and affordable method for K_{eo} measurement. We also present numerical values for K_{eo}, with a conscious quantification of uncertainties, for three different substrates with frequent use in e-µPADs : Whatman #1, S&S, and Muntktell 00A filter paper. Besides the numerical values obtained for uncertainties a discussion is included to identify and quantify possible deviations from the linear model in terms of evaporation and viscosity changes due to the heating by Joule effect of the substrates. We also provide equivalent values for ζ_p, by using the model presented in [12] and finally gather such information with previously reported values in order to provide readers for the first time (to the best of our knowledge) with a reliable compilation of ζ_p values for the most frequently used substrates. The presented EOF measurement method as well as the numerical values obtained will endow developers with reliable data, which will allow rational design of e-µPADs, needed to tackle new applications in sensitive fields like POC or food safety.

2 Materials and methods

2.1 Buffer solutions

In order to keep pH values constant during measurements Tris acetate (12 mM Tris - 22 mM acetic acid, pH=4.78), Tris phosphate (6.3 mM Tris - 4 mM phosphoric acid, pH=7.02), and Ammonium acetate (7 mM ammonium - 3.5 mM acetic acid, pH=9.29) were used as BGEs. All compounds were purchased from Laboratorios Cicarelli (Reagent SA, San Lorenzo, Argentina). All solutions were prepared with ultra pure water obtained from an inverse osmosis purifier (Osmoion, Apema SRL, Villa Dominico Argentina). bsphackesphack The pH and conductivity of solutions were corroborated with ph-Meter (Adwa A12, Szeged, Hungary) and conductivity meter (Adwa AD 203, Szeged,Hungary).

2.2 Experimental setup

The proposed setup is based on the gravimetric measurement of the electroosmotic flow in a paper strip placed over two parallel blades in the arrangement shown in the Fig. 1. Here, the middle blade is attached to a fixed support and the left blade is placed over a precision scale (Ohaus Pioneer, Parsippany, NJ, USA). The scale records the change of mass distribution produced by the EOF. This scheme amplifies the force over the scale and balances the effects of evaporation, as will be explained in the next section. More graphical details about the setup and connections can be found in the supporting information.

Paper strips were cut from disks (Whatman #1, grade No. 1, 120 mm discs; Munktell, 00A, 125 mm discs; S&S, 0859, 150 mm discs) into 58 mm long (L_{tot}) and 20 mm width (w) pieces following the machine direction [23]. Devices were fabricated by laser-cutting (40W CO_2 laser from Lasers Cuyana, San Rafael, Argentina) and hot lamination (DASA LM330) on both sides of the paper strip. At both ends, symmetric 9 mm space was intentionally left for the liquid reservoirs by using a shorter lamination pouch on one side. Paper channels were laminated using film pouches of 150 µm thick (Binderplus, China) at 130 °C, at constant speed of 3.5 mm/s. The back of the strip was attached to hydrophobic double-sided adhesive tape (Stiko, Silkstone SA, Buenos Aires, Argentina), and placed over a glass slide settled on the top of the two thin blades, following the scheme in Fig. 1A.n

Electric potential on the range of $\pm\ 100 - 500\,\text{V}$ were applied across the reservoirs by using two platinum electrodes keeping minimum contact ~~in contact only~~ with the liquid in the reservoirs

to minimize interference from buoyancy forces. It was supplied by a computer controlled electric source (Keithley 6487 Picoammetter, Cleveland, OH, USA). This instrument can measure the applied current, which allows estimating the electrical resistance of the circuit as a function of time. The polarity was inverted periodically after 50 s in order to balance residual evaporation effects (see next section), but also possible redox effects on electrode surface, such as bubble formation or electrolyte exhaustion, among others. Temperature measurements were performed with an infrared thermometer Testo 805i (Neustadt, Germany). Mass measurement experiments were repeated at least three times. Each experiment involved 6 to 10 voltage cycles. The scale digital output was analyzed by using the open source tool GNU Octave [24].

2.3 Measuring principle

The stability of the glass slide in Fig. 1 requires a zero net sum of the moments with respect to the fixed support:

$$F_1 L_1 - F_2 L_2 - R_s d_s = 0$$

where F_1 and F_2 are the liquid weight in reservoir 1 and 2 respectively, R_s is the force measured by the scale, and L_1 and L_2 are the lengths measured from the center of mass of each reservoir to the fixed support (See Fig. 1). In this equilibrium equation, the torque contributions of the paper strip, double-sided adhesive tape and the glass slide are not considered as they do not change their contribution during the measurement process.

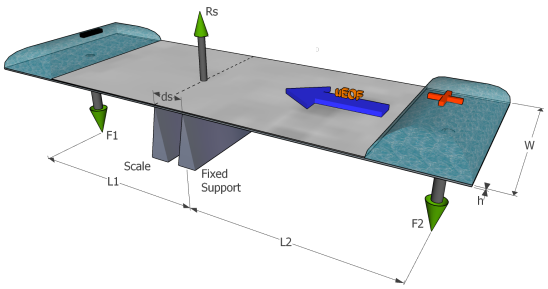

Figure 1: Experimental setup used to measure EOF on paper substrates. A scale and a fixed support holds the paper strip. Minus (black) and plus (red) signs indicate a possible configuration for applying electric potential at reservoirs R_1 and R_2, respectively, generating EOF in the direction indicated by the blue arrow. This direction is alternated over the experiments as it is described in section 2.5.

When a positive electric potential difference $\Delta\Phi$ is applied between reservoirs 1 and 2, after a time period Δt, a mass fraction Δm moves from reservoir 2 to reservoir 1. In this condition, a new equilibrium situation is reached, i.e.:

$$(F_1 - g\Delta m)L_1 - (F_2 + g\Delta m)L_2 - R_s^{'} d_s = 0$$

where $R_s^{'}$ is the new force measured in the scale. In this way, the variation in the scale $R_s^{'} - R_s = \Delta R_s$ can be calculated as:

$$\Delta R_s = g\Delta m \frac{L_1 + L_2}{d_s} = g\Delta m \frac{L}{d_s}. \tag{4}$$

Since $g\Delta m$ is the force value that the balance would record when measuring a mass Δm, i.e. the weight of Δm, the ratio L/d_s results in an amplification factor of the measured weight. In our experiments this factor is approximately 25. Simultaneously, this experimental layout allows self-compensation of the mass variations at the reservoirs due to evaporation. Actually, if a mass quantity Δm_e is evaporated *simultaneously* at each reservoir, the scale measurement variation will be:

$$\Delta R_s = g\Delta m_e \frac{L_1 - L_2}{d_s}. \tag{5}$$

In this way, by choosing L_1 similar to L_2 by symmetrically placing the reservoirs around the fixed support, the variations due to evaporation can be canceled out. In any case, if any asymmetry still persists, it is expected a constant change of the scale measure. If the direction of the EOF is periodically reversed (changing the polarity of the potential), then it is possible to subtract this effect from the measurements, as it is shown in the next section.

The electroosmotic volume flow rate Q_{EOF} and Δm are related through density ρ, i.e. $\Delta m = \rho Q_{EOF} \Delta t$; where $Q_{EOF} = u_{EOF} w h$ with h being the thickness of the paper strip. Combining these definitions, eq. (4), and using $\Delta m = \Delta R_s / g$ one finally obtain,

$$u_{EOF} = \frac{\Delta m d_s}{w h \rho \Delta t L} \tag{6}$$

2.4 Calibration

The calibration procedure presented in this section is meant to obtain the amplification factor L/d_s shown in eq. (4). This coefficient could be calculated by direct measure of the distances involved, however this will introduce a new error, since L_1 and L_2 are measured from the fixed support to the center of mass of the drops on the reservoirs. Here we propose a simple method to overcome this issue. Initially, the glass slide is placed in position (i.e: the center of gravity of the slide between the fixed support and the scale); once equilibrium is achieved, a buffer solution drop of mass m_0 is released on reservoir 1, noticing a change in the scale of mass $\Delta m_1 = m_0 \cdot L_1/d_s$. At this time, the liquid starts to flow in direction to reservoir 2. When the fluid front reaches the end of the laminated paper strip, a second drop of mass m_0 is released on reservoir 2, with a consequent change of magnitude $\Delta m_2 = -m_0 \cdot L_2/d_s$. In this case the force on the scale decreases, given the relative position of the reservoir 2 to the fixed support (See Fig. 1).

Taking into account the mass change values obtained during the calibration procedure, the amplification factor can be readily obtained as,

$$L/d_s = \frac{\Delta m_1 - \Delta m_2}{m_0} \tag{7}$$

In the experiments, the mass of the drops used at calibration, m_0, was approximately 200 µg, corresponding to a solution volume of 200 µL. Distances (L_1 and L_2) from the center of mass of each reservoir to the fixed support were about 25 mm The distance between blades was approximately 2 mm, resulting in an amplification factor of approximately 25.

It is important to note that it is assumed that throughout the measurement process, the center of mass of the liquid in the reservoirs does not change its position. This hypothesis is reasonable since the shape of the liquid does not change substantially due to evaporation.

2.5 Data processing

Data acquired from mass measurements is processed in order to calculate the mass change ratio $\Delta m/\Delta t$ from eq. (6) to finally calculate K_{eo} by means of eq. (1). Fig. 2A shows the mass evolution obtained for a typical measurement using Whatman #1 paper at $pH = 4.78$, alternating $\Delta\Phi = \pm$ 300 [V] every $\Delta t = 50s$. It is worth to note the positive and negative slopes after a Δt period, which correspond to the polarity inversion of $\Delta\Phi$. Taking relative peak points at regular interval of Δt, Δm can be precisely accounted for.

Data series with positive and negative slopes are averaged separately and later combined to obtain a single value. This procedure corrects the mass drift found in each experiment. A linear trend is used to fit data-points. The initial and final 5 % of the signal is not considered to avoid noisy data obtained around the abrupt voltage changes (inset in Fig. 2A). These sharp peaks are produced by small bubbles detached from electrode surface generating a detectable force that is measured by the scale.

In addition to the mass drift, Fig. 2 shows a similar effect over the electric resistance, which exhibits a decay (Fig. 2B). Electric resistance has a transitory phase due to the reconfiguration of the electrical double layer at electrode surfaces (resistance downward sharp peaks in Fig. 2B). It is worth to mention that the described sharp transitory effects are kept out of the measurement results as far as they occur in a region that is not considered for calculation.

The decay effects over mass and resistance measurements will be discussed in section 3.3. Finally, weighted arithmetic mean is used to estimate the u_{EOF} for each pH value.

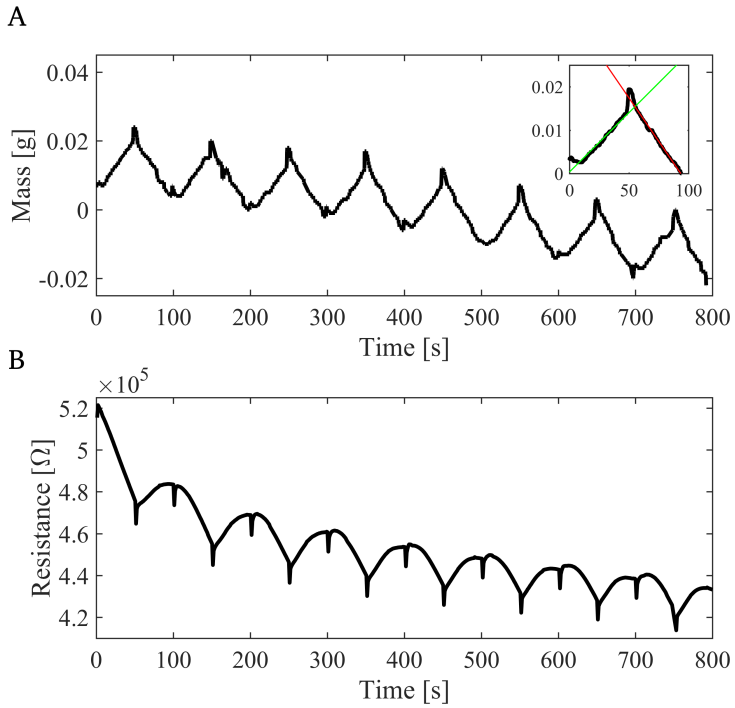

Figure 2: Scale lecture (A), and electrical resistance (B) as function of time for Tris-Acetic, $pH = 4.78$, $\Delta\Phi = \pm\ 300$ [V] and $\Delta t = 50s$, for Whatman #1 . The linear fit for averaged mass signal is shown in the inset.

3 Results and discussion

3.1 Electroosmotic flow measurements

Fig. 3 gathers the main results obtained with the presented experimental method, showing the measured electroosmotic velocity and mobility as a function of electric potential for the three different values of pH, in Whatman #1 paper. A remarkable linearity is shown for low electric potential values, which reinforces the model presented in eq. (3). In contrast, linearity decreases with high potential values, and the possible causes for this deviation are discussed in section 3.3.

3.2 K_{eo} and zeta potential calculations

Table 1 presents the results obtained for K_{eo} and ζ_p by using eqs. (1) and (3), respectively. Reported values for K_{eo} were corrected from the deviations of the linear model, by considering the temperature increase due to Joule effect, with its consequent influence over the viscosity. Such influence simultaneously affects electrical and rheological parameters of the system. The reported values of K_{eo} obtained at room temperature (K_{eo0}) are obtained from fitting the experimental data with a model of heating by Joule effect. This model is discussed in section 3.3.2.

For the calculation of ζ_p by applying eq. (3), $\tau = 2.9$ was considered [12] for all substrates due to the high uncertainty in literature about this parameter. Reliable and robust measurements of τ will be part of a future work. Substrate porosity was found by weighting dry and wet substrates with known geometries. As far as aqueous diluted solutions were used, we considered $\mu = 1.0\,\mathrm{mPa\,s}$ at initial 23 °C and a relative permittivity $\epsilon = 7.08 \times 10^{-10}\,\mathrm{C^2/Nm^2}$.

Finally, the obtained values for ζ_p were gathered with other values obtained from literature in Fig. 4. This figure reflects the reliability and robustness of the proposed method by considering the magnitude of the error bars, but also the monotonicity of the measured values with pH. The behaviour of the other measured substrates is similar, i.e. K_{eo} and ζ_p increase with pH, with higher influence of pH for S&S, moderate for Whatman #1, and very stable conditions for Muntktell 00A. In terms of magnitude of the flow S&S paper exhibits a very low K_{eo} which makes it suitable for applications that require EOF cancellation or minimization. In the case of Muntktell 00A, its stability over pH offers good oportunities to implement techniques with broad pH range operations

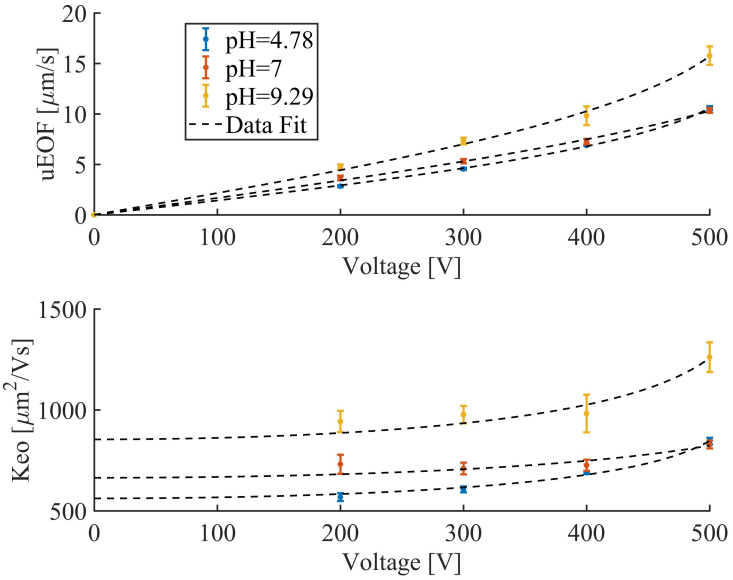

Figure 3: Measured electroosmotic velocity (A) and electroosmotic mobility (B) for different electric potentials using buffer solutions with variable pH in Whatman #1. Data fit corresponds to eq (11), where K_{eo} is modeled using the non-linear model described in section 3.3.2.Uncertainty values represent the 95 % confidence intervals on the mean using a Student-t distribution.

	ϕ	pH	K_{eo0} [$\frac{\mu m^2}{Vs}$]	ζ_p [mV]
Whatman #1	0.69	4.78	561 ± 22	−11.8 ± 0.5
		7	664 ± 65	−13.9 ± 1.4
		9.29	854 ± 92	−17.9 ± 1.9
Munktell 00A	0.47	4.78	537 ± 95	−16.6 ± 2.9
		7	549 ± 40	−16.9 ± 1.2
		9.29	512 ± 68	−15.8 ± 2.1
S&S	0.42	4.78	81 ± 35	−2.7 ± 1.2
		7	214 ± 52	−7.3 ± 1.8
		9.29	258 ± 56	−8.8 ± 1.9

Table 1: ζ_p potentials and K_{eo0} obtained for different buffer solutions and types of substrates used. Uncertainty values were calculated by using 95 % confidence bounds in fit process by using eq. 11

such as IEF. Finally, Whatman # 1 paper offers a similar behaviour to closed channel materials such as glass or hydrophylic PDMS, working as a good starting point for adapting traditional electrophoretic separations to paper-based substrates.

It is worth to mention here that the reported values for K_{eo0} and ζ_p correspond to those measured with pouch laminated paper substrates to minimize evaporation effects as far it is recommendable for improving reproducibility. These reported values can be slightly modified when working with bare substrates (without lamination) or different lamination materials, due to the fact that lamination has a limited influence over the total fiber free surface that allocates electrical double layer producing EOF.

3.3 Deviations from linear model

In order to account for possible error sources which deviate the obtained experimental values from the linear model, in the following we describe different effects that are present in the setup affecting the measurement process. We discuss also how to tackle or quantify such effects for improving future setups.

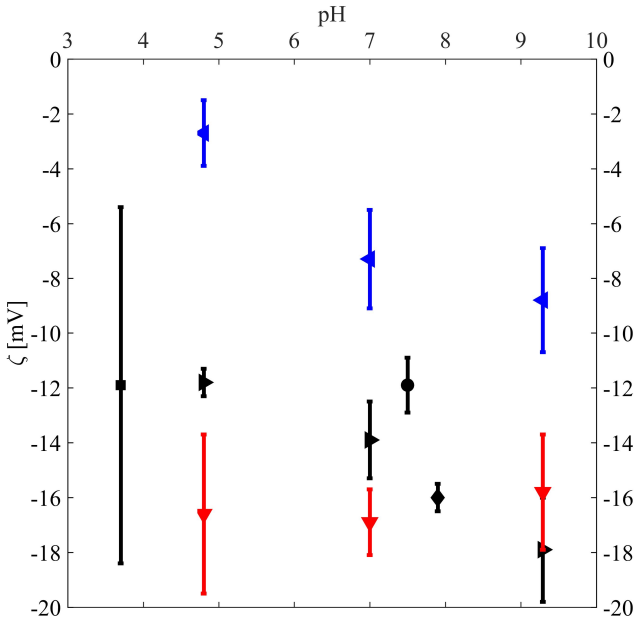

Figure 4: $\zeta_p(pH)$ values for different substrates. Square (■ [20]) circular (● [21]) and rhomboidal (♦ [22]) markers correspond to results obtained for Whatman#1 starting from bibliography data. Triangular markers correspond to estimations performed with experimental data obtained in this work for different paper types: Whatman #1 (►), Munktell 00A (▼) and S&S (◄).

3.3.1 Evaporation

Evaporation is an important effect to consider in measurements. It reduces reservoir volume with time and affects measurements. However, the presented setup self-compensates the evaporation effect as it was already discussed in section 2.3. However, such effect can be quantified in a calibration procedure by measuring the slope after the wetting front reaches the end of the paper strip and waiting for the pores of the paper strip to be fully saturated as was described in section 2.4. Evaporation symmetrically affects both reservoirs, consequently, the scale will not register any changes in this configuration. Nevertheless, a small effect is still present due to a possible asymmetry of the relative reservoir positions relative to the fixed support. This residual asymmetry is corrected by averaging positive and negative slopes as it is shown in Fig. 2A and its inset.

3.3.2 Conductivity drift and Joule effect

In Fig. 2B the electric resistance over time is shown for $\Delta\Phi = 300\,\mathrm{V}$ inverted periodically every 50 s. It can be seen there that the average value is decreasing over time. On a general basis, such resistance is given by:

$$R_p = \frac{1}{\sigma_p}\frac{L}{A_p} \tag{8}$$

where subscript p refers to paper, A_p is the cross-sectional area and σ_p the electric conductivity. Therefore, the time-dependent variations observed in Fig. 2B can be explained only through changes in L, A_p or σ_p. Assuming that L and A_p are constant parameters over long time periods, focus must be put on σ_p changes. For a paper substrate, completely wet with an electrolyte solution, σ_p can be calculated as [12]:

$$\sigma_p = F\sum_{j=1}^{N} z_j^2 \frac{\Omega^j}{\tau^2} C^j \phi \tag{9}$$

where F is the Faraday constant, Ω^j the electrophoretic mobility, z^j the charge number and C^j concentration of the $j-$th species, respectively. By assuming a buffered system, C^j is constant and

the only variable parameter in eq. (9) is Ω^j. If j is a small ion, a possible model for Ω^j [16] is:

$$\Omega^j = \frac{q^j}{6\pi\mu r_s^j} \tag{10}$$

where q^j is the charge, r_s^j is the hydrodynamic radius related to the size of the j-hydrated molecule. Again, from this expression, the only parameter than can change its value over time is μ. The decay observed in the electric resistance as it is shown in Fig. 2B must be due to the decrease of the viscosity of the solution, due to thermal heating produced by Joule effect. Considering the electric current and potential measured during the experiments, this effect is not negligible.

The power of heating is $P = \frac{V^2}{R_p}$ and it depends on σ_p for each buffer solution. The maximum value for P can reach up to $1\,\mathrm{W}$ at $\Delta\Phi = 500V$. Such heating produces changes in bulk fluid viscosity that are consistent with changes in electric conductivity. For example, surface temperature measurements made in Munktell filter paper using an infrared thermometer, shows that for $\Delta\Phi = 400V$, the temperature change is $\Delta T \approx 22\,^{\circ}\mathrm{C}$. In this process, the electric resistance varies from $2.84 \times 10^5\,\Omega$ to $1.88 \times 10^5\,\Omega$ respectively, obtaining a variation ratio of 0.66. Such ratio is consistent with the expected decrease of the viscosity for the measured temperature range [25].

As far as the temperature increase reduces the buffer solution viscosity and this in turn bsphack-esphack produces the non-linear behavior of u_{EOF} showed in Fig. 3 at high voltage values. In order to quantify this effect, a physical model that accounts for variations in rheological and electrical properties of the electrolyte was developed. In the following, the main results for such model are provided. Full hypotheses discussion and mathematical details can be found in the supporting information.

Based on such model, the final expression for K_{eo}, related to the electric potential is:

$$K_{eo} = \frac{2K_{eo_0}}{1 + \sqrt{1 - \alpha\Delta\Phi^2}} \tag{11}$$

The values reported in Table 1 were obtained by using this model to fit data shown in Figure 3. Here, the parameter α gathers the thermal characteristics of the strip and electrical properties of the buffer solution that determine the thermal behavior of the system, it can be calculated as:

$$\alpha = \frac{4A}{Lwh'R_0} \tag{12}$$

where A measures the relative viscosity variation dependence with the solution temperature (about $0.024\,\mathrm{K}^{-1}$ [25] at ambient temperature), L and w are geometrical dimensions of the paper strip (see Fig.1), R_0 is the electrical resistance at room temperature and h' is the convective heat transfer coefficient. As it was mentioned, the parameter α characterize, the system both in terms of heat generation (due to Joule effect, through R_0), but also in terms of heat dissipation capacity of the strip (through h' and the rest of the parameters).

The values of α obtained from fitting the experimental data are in the range of 2.5×10^{-6} - $3.5 \times 10^{-6}\,\mathrm{V}^{-2}$. This values are consistent with the experimental value found for h' of about $68 \pm 15\,\mathrm{W/m^2K}$ and measured values of R_0 around $0.5\,\mathrm{M\Omega}$. More details about this calculations can be found in the supporting information.

4 Concluding remarks

In this work, a novel measurement method for K_{eo} has been developed in order to tackle the lack of information for developing robust and rational e-µPADs design. It has been demonstrated along the paper that such method is robust, reliable, and affordable. Such robustness is partially based on the fact that the setup auto-calibrates and self-compensates evaporation effects. All experiments demonstrate to be reproducible with remarkable low scatter when compared to previous works on e-µPADs. The experimental results obtained for K_{eo} are independent of the applied voltage for moderate field values. For high field values, Joule heating must be taken into account, and it was found that the variation in the value of measured K_{eo} can be explained in a consistent way with the decrease in the viscosity of the solution due to temperature increase. A model has been proposed to describe the dependence K_{eo} with the applied voltage, finding ~~an excellent~~ proper correlation

with the experimental data. From the obtained K_{eo} we derived $\zeta_p(pH)$ values that are consistent with those previously reported in the bibliography. Moreover, these K_{eo} and ζ_p values allow data driven decision making. For example, a e-µPAD designer might choose Munktell 00A paper, with an almost constant $K_{eo}(pH)$, if the pH of the solution is unknown or it is expected to change, but still wants to keep EOF constant. Alternatively, Whatman #1 might be preferred over S&S paper if higher EOF is required. Finally, we consider that this method is straightforward to be reproduced for other groups devoted to e-µPADs development for the different paper or paper like substrates used in the wide application field of such devices.

Acknowledgments

We thank Dr. Luciana Vera Candioti for her advises about BGEs. This research was supported by ANPCyT (GrantPICT-2018-02920), UTN (Grant PID ASUTIFE0005525TC) and CONICET, Argentina.

Conflict of interest statement

All authors declare complete absence of financial/commercial conflicts of interest.

References

[1] Salentijn, G. I., Grajewski, M., and Verpoorte, E. Anal Chem, 2018, 90, 13815–13825.

[2] Cremer, H., Tiselius, A., et al. Biochem. Ztschr., 1950, 320, 273–283.

[3] Kunkel, H. G. and Tiselius, A. J Gen Physiol, 1951, 35, 89–118.

[4] Durrum, E. L. J Am Chem Soc, 1951, 73, 4875–4880.

[5] Grassmann, W. and Hannig, K. Naturwissenschaften, 1950, 37, 397–397.

[6] Ge, L., Wang, S., Ge, S., Yu, J., Yan, M., Li, N., and Huang, J. Chem Commun, 2014, 50, 5699–5702.

[7] Xu, C., Lin, W., and Cai, L. J Chem Educ, 2016, 93, 903–905.

[8] Chagas, C. L., deSouza, F. R., Cardoso, T. M., Moreira, R. C., daSilva, J. A., deJesus, D. P., and Coltro, W. K. Anal Methods-UK, 2016, 8, 6682–6686.

[9] Moghadam, B. Y., Connelly, K. T., and Posner, J. D. Anal. Chem., 2014, 86, 5829–5837.

[10] Rosenfeld, T. and Bercovici, M. Lab Chip, 2014, 14, 4465–4474.

[11] Schaumburg, F., Kler, P. A., Carrell, C. S., Berli, C. L., and Henry, C. S. Electrophoresis, 2020, 41, 526–569.

[12] Schaumburg, F., Kler, P. A., and Berli, C. L. Electrophoresis, 2020, 41, 598–606.

[13] Urteaga, R., Elizalde, E., and Berli, C. L. Analyst, 2018, 143, 2259–2266.

[14] Mirzadeh, M., Zhou, T., Amooie, M. A., Fraggedakis, D., Ferguson, T. R., and Bazant, M. Z. arXiv preprint arXiv:2003.05974, 2020.

[15] Yao, S. and Santiago, J. G. J Colloid Interf Sci, 2003, 268, 133–142.

[16] Probstein, R. Physicochemical Hydrodynamics. An Introduction. Wiley-Interscience, 2nd edition, 2003.

[17] Berli, C. L. A., Piaggio, M., and Deiber, J. Electrophoresis, 2003, 24, 1587–1595.

[18] Damián, S. M., Schaumburg, F., and Kler, P. A. Comput Phys Commun, 2019, 237, 244–252.

[19] Rosenfeld, T. and Bercovici, M. Lab Chip, 2019, 19, 328–334.

[20] Leung, V., Shehata, A.-A. M., Filipe, C. D., and Pelton, R. Colloid Surf A, 2010, 364, 16–18.

[21] Mettakoonpitak, J. and Henry, C. S. Sensor Actuat B-Chem, 2018, 273, 1022–1028.

[22] Schaumburg, F., Carrell, C., and Henry, C. S. Anal Chem, 2019.

[23] Elizalde, E., Urteaga, R., and Berli, C. L. A. Microfluid Nanofluid, 2016, 20.

[24] GNU Octave Online. 2020. Accessed: 2019-07-10.

[25] Huber, M., Perkins, R., Laesecke, A., Friend, D., Sengers, J., Assael, M., Metaxa, I., Vogel, E., Mareš, R., and Miyagawa, K. J Phys Chem Ref Data, 06 2009, 38, 101–125.